Simulation of the radiative control and QSF configuration on EAST by the SOLEDGE2D-EIRENE code

K. Wu[1,2,3], P. Innocente[4], G. Calabrò[1], B. J. Xiao[2,3], Z. P. Luo[3]

[1]*Department of Economics, Engineering, Society and Business Organization (DEIm), University of Tuscia, Viterbo, Via del paradiso, 47, 01100, Italy*

[2]*University of Science and Technology in China, Jinzhai Road 59, 230031, Hefei, China*

[3]*Institute of Plasma Physics, Chinese Academy of Sciences, Shushanhu Road 350, 230031, Hefei, China*

[4] *Consorzio RFX, Corso Stati Uniti 4, 35127, Padova, Italy*

Abstract

In order to analyze the transfer process in scrape-off layer (SOL) and radiative control scenario on EAST by impurity seeding, we have used the edge code SOLEDGE2D-EIRNE to model two typical H-mode upper-single null (USN) discharges. Modeling results confirm that neon gas injection contributes to the reduction of the divertor peak power fluxes, which is consistent with the Langmuir probe (LP) data but does not provide the nearly uniform radiation increment in the core. Based on the simulation of a non-seeded EAST quasi-snowflake (QSF) plasma, a prediction of the neon seeding phase with the same configuration is done.

1. Introduction

The transport processes in SOL result in the plasma-wall interactions (PWIs) and make the plasma facing components (PFCs) sustain the continuous power flux strikes [1]. The transport code SOLEDGE2D-EIRENE is a simulation code for the edge plasma modeling [2]. The penalization technique is used into SOLEDGE2D-EIRENE to treat the different boundary geometry conditions and magnetic configurations [3]. EAST is a superconducting tokamak with ITER-like tungsten (W) divertor. Recently, EAST has built the feedback control system of the radiated power [4] and also achieved the quasi-snowflake (QSF) discharges [5]. In this paper, we firstly use SOLEDGE2D-EIRENE to simulate the EAST seeded plasmas in USN configuration and then analyze seeding applied to QSF configurations.

2. Experimental setup and the main diagnostics

The experimental conditions are almost same for these two analyzed USN plasmas. Both them are in H-mode and the plasma current $I_p = 0.4MA$. The pulse #71019 is in the radiation feedback control scenario. Ne gas is seeded for a pulse length 100ms in the feedforward (FF) control phase from the puffing valve at the upper inner divertor at 3.0 s shown in figure 1(c), the puffing gas flux $\Gamma_{UIV} \approx 4 \times 10^{20} s^{-1}$. Instead, shot #71022 has no impurity seeding. QSF shot #71468 is in different experimental conditions with plasma current $I_p = 0.25MA$, and $n_e \approx 4 \times 10^{19} m^{-3}$. All these discharges have the same drift direction $B \times \nabla B \downarrow$. The radiated power is measured by the AXUV array [6]. The EAST Langmuir probe arrays are installed on all the four divertor target plates to provide the data of particle and power fluxes [7].

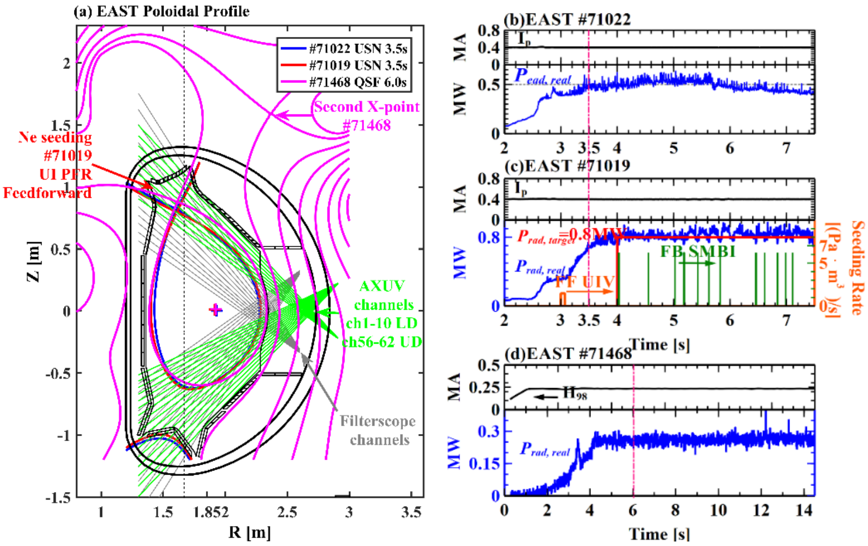

Figure 1. (a) the LCFS of the above three EAST shots in the relative time point, the second X-point of #71468 is also shown. The green lines represent the AXUV channels covering the divertor regions. (b) (c) (d) the time slice of the plasma current (black line) and the radiated power (blue line). In figure (c), the feedforward Ne pulse is in orange line, written as FF UIV (feedforward upper inner valve). The dashed-dot line indicates the time point in the simulations.

3. Modeling results

3.1 USN plasmas with Ne seeding

Table 1 shows the main cross-field transport parameters for the two USN simulations.

Table 1. Transport parameters in USN simulations.

Parameters	$D_{\perp,e\&i}\ [m^2 s^{-1}]$	$\nu_{\perp,e\&i}[m^2 s^{-1}]$	$\chi_{\perp,e\&i}[m^2 s^{-1}]$	$P_{in}[MW]$
#71022	1.8	1.8	1.0	1.78
#71019	1.5	1.5	1.0	1.96

For the shot #71019, after Ne seeding, the plasma radiated power is increased in different regions. The experimental data before neon seeding shows a nearly uniform distribution in the main plasma and divertor region. The increment of the radiated emission caused by Ne seeding is also uniform as shown in figure 2. This kind of distribution and increment can be caused by various factors. The low edge electron temperature T_e at the outer mid plane separatrix is one of the possible reasons to allow more Ne particles into separatrix. In the modeling results, the OMP edge T_e is in the range of ~76-90 eV, the peak value of the Ne radiation power loss function is not in this region (~50eV), and the Ne impurity alone cannot supply the strong (beyond 50% total radiation) increment of the core radiation. In the same radiation control experimental campaign, a slight increment of W line emission is measured during Ne seeding in another pulse [4], which indicates that a few of W influx is in the main plasma after Ne seeding and partly contributes to the core radiation. However, whether the neon seeding indeed cause the additional sputter of W still needs more study.

The SOLEDGE2D-EIRENE cannot simulate the whole core plasma, so the modeling radiated power is mainly from edge plasma as shown in figure 1(a) green lines. Modeling result is consistent with the AXUV measurement in the edge region as shown in figure 3. Based on this result, the radiated power in the divertor region is about 0.23MW, only 25.6% of the total radiated power, showing that there is still an improving margin. The simulated data of the divertor power fluxes are almost same to the Langmuir probe measurement as shown in figure 4. The additional Ne seeding provides the reduction of the divertor peak power fluxes by about $0.15MW/m^2$. The peak T_e also declined 10eV. It should be mentioned that the current result still can be improved, a bigger Ne injecting volume may achieve a better mitigation effect.

3.2 QSF plasmas with Ne seeding

The same transport parameters and an additional Ne are added into QSF #71468 to compare the difference with impurity seeding between USN and QSF shape. Because the QSF discharge has higher input power (~2.6MW) and lower I_p, the edge conditions are different. The higher OMP T_e (beyond 100eV) makes the Ne particles hard to penetrate the LCFS, and at this temperature range, the power loss function of Ne is small. Thus, the radiated power in QSF simulation is far below the USN level compared to the USN situation (Figure 5(a)), and the radiation is focused on the common flux surface of the upper outer divertor region as shown in figure 5(b). Whether this kind of distribution is related to the QSF shape still needs more study to determine.

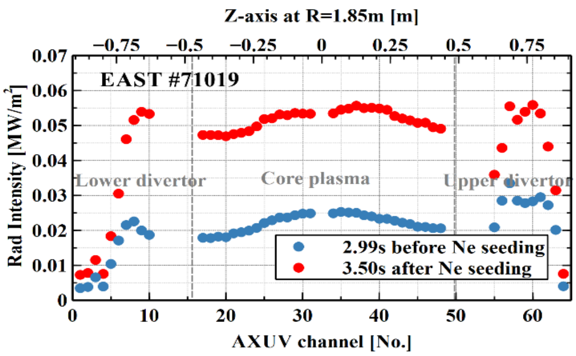

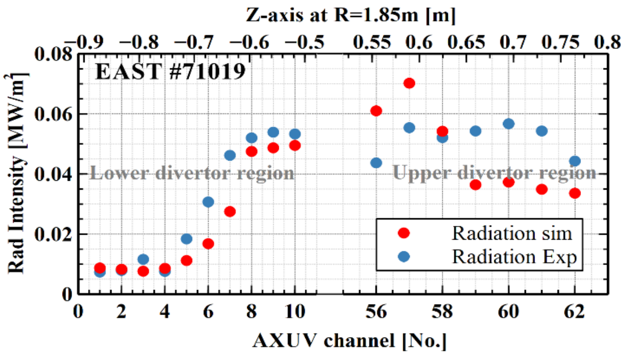

Figure 2. The radiation increments at different region after Ne seeding in #71019.

Figure 3. The comparison of the edge radiation at different position between modeling and diagnostic in #71019 at 3.5s.

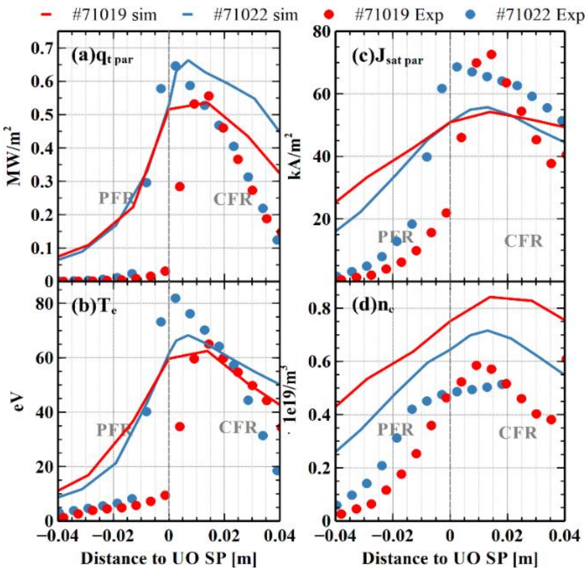

Figure 4. The simulation (line) and diagnostic (dot) data of the divertor parameters. (a) parallel heat flux; (b) electrical temperature; (c) saturation ion current; (d) electron density in #71019 (red) and #71022 (blue).

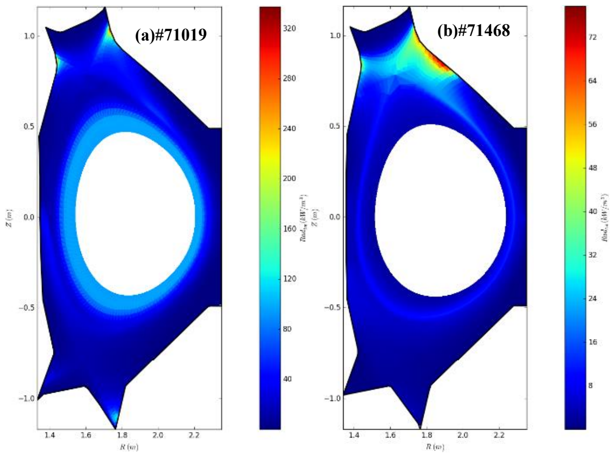

Figure 5. The 2D distribution of the radiated power in the SOLEDGE2D-EIRENE simulation. (a) USN 71019 with neon seeding; (b) QSF 71468 with neon seeding. More radiation in QSF shape located in the UO divertor.

4. Conclusions

We used the SOLEDGE2D-EIRENE to model the USN plasma on EAST with impurity seeding. The modeling results of the edge radiation and divertor power fluxes are consistent with the diagnostic data. The additional Ne seeding indeed lower the divertor peak power flux. The uniform increment of the radiated power in the main plasma and divertor region still needs more research. The QSF plasma with Ne impurity is also simulated. In the preliminary result, the QSF shape has an impact on the radiation distribution, which is different to that in USN shape.

Reference

[1] M. Wischmeier et al., J. Nucl. Mater., 463 (2015) 22

[2] H. Bufferand et al., J. Nucl. Mater. 438 (2013) S445

[3] H. Bufferand et al., Nucl. Fusion 55 (2015) 053025

[4] K. Wu et al., Nucl. Fusion 58 (2018) 056019

[5] G. Calabrò et al., Nucl. Fusion 55 (2015) 083005

[6] Y. M. Duan et al., J. Nucl. Mater., 438 (2013) S338

[7] J. C. Xu et al., Rev. Sci. Instrum., 87 (2016) 083504